land

MDPI

Article

Machine Learning-Based Assessment of Land-Use Change, Forest Recovery, and Landscape Connectivity in Islamabad

Muhammad Tariq Badshah [1], Hakim Ullah Khan [1,2], Muhammad Shabir [3], Shahid Rahman [3], Khadim Hussain [1,4], Farhan Amin [5,*], Isabel De la Torre Díez [6], Mirtha Silvana Garat de Marin [7] and Eduardo Silva Alvarado [8]

1 Research Center of Forest Management Engineering of National Forestry and Grassland Administration, Beijing Forestry University, Beijing 100083, China; badshahgi90@gmail.com (M.T.B.); hakimullah201@yahoo.com (H.U.K.); khadimfr49@gmail.com (K.H.)
2 School of Soil and Water Conservation, Beijing Forestry University, No. 35 Tsinghua East Road, Haidian District, Beijing 100083, China
3 Department of Computer Science, University of Buner, Buner 19290, KPK, Pakistan; sabirshah@ubuner.edu.pk (M.S.); rahmanshahid059@gmail.com (S.R.)
4 Institute of Geographic Sciences and Natural Resources Research, Chinese Academy of Sciences, Chaoyang, Beijing 100101, China
5 School of Computer Science and Engineering, Yeungnam University, Gyeongsan 38541, Republic of Korea
6 EHealth and Telemedicine Group, University of Valladolid, 47011 Valladolid, Spain; isator@uva.es
7 Department of Projects, Universidad Internacional Iberoamericana, Arecibo, PR 00613, USA; silvana.marin@unic.co.ao
8 Department of Projects, Universidad Europea Del Atlántico, Isabel Torres 21, 39011 Santander, Spain; eduardo.silva@uneatlantico.es
* Correspondence: farhanamin10@hotmail.com

Abstract

LULCC is a major driver of habitat fragmentation, biodiversity loss, and declining landscape connectivity, particularly in rapidly urbanizing regions. Although Islamabad has experienced substantial urban expansion and forest-cover change, long-term city-scale assessments linking land-cover dynamics with landscape connectivity remain limited. This study examined spatiotemporal LULCC in Islamabad from 1991 to 2021 and assessed whether recent forest recovery improved landscape structural connectivity. Landsat images acquired in 1991, 2001, 2011, and 2021 were classified into five land-cover categories: water, forest, built-up area, bare land, and agricultural land. Classification was performed using the Random Forest (RF) algorithm in Google Earth Engine (GEE). Landscape composition and spatial configuration were quantified using FRAGSTATS 4.3, while forest fragmentation was evaluated using the Landscape Fragmentation Tool v2.0 (LFT) with a 100 m edge threshold. The classifications achieved overall accuracies above 90%, with Kappa coefficients (K) greater than 0.85. Built-up area increased from 76.31 km^2, representing 7.55% of the study area, in 1991, to 258.62 km^2, or 25.60%, in 2021, demonstrating rapid urban expansion and associated habitat conversion. Forest cover increased to 340.86 km^2 in 2001, declined to 271.96 km^2 in 2011, and subsequently recovered to 409.22 km^2 in 2021. Despite this increase in forest extent, fragmentation metrics indicated persistent spatial subdivision and limited structural connectivity. High patch density (PD), reduced landscape aggregation, and changes in the largest patch index (LPI) indicated persistent spatial subdivision and limited habitat continuity. These findings highlight the value of integrating RF-based land-cover classification, multitemporal remote sensing, and landscape metrics for urban environmental monitoring. The findings suggest that future land-use planning should consider landscape connectivity, protection of existing forest patches, and spatially coordinated restoration alongside continued reforestation.

Check for updates

Academic Editor: Mark Altaweel

Received: 10 August 2026
Revised: 31 August 2026
Accepted: 1 September 2026
Published: 4 September 2026

Copyright: © 2026 by the authors. Licensee MDPI, Basel, Switzerland. This article is an open access article distributed under the terms and conditions of the Creative Commons Attribution (CC BY) license.

Keywords: urban sprawl; land use and land cover (LULC) change; landscape metrics; Islamabad

1. Introduction

Land-use and land-cover change (LULCC) is among the most pervasive manifestations of human influence on the Earth's surface. It alters landscape structure, ecosystem functioning, biodiversity, ecosystem services, and human well-being [1]. Since the 1990s, LULCC has become a major focus of global environmental research because of its effects on landscape composition, spatial configuration, and ecological stability [2]. Land cover refers to the observable biophysical characteristics of the Earth's surface, whereas land use describes the human activities and interventions that modify those characteristics [3]. Examining both dimensions is therefore necessary to understand how anthropogenic pressures transform natural and managed landscapes. Landscape pattern describes the spatial composition and configuration of landscape elements and reflects the heterogeneity generated by natural processes and human activities [4,5]. Changes in these patterns can modify habitat availability, patch isolation, edge conditions, and ecological continuity. Assessing landscape structure is consequently essential for determining whether land-cover transitions support or undermine ecological sustainability. The rapid conversion of forests and agricultural land into built-up and industrial areas has accelerated in many regions, particularly around expanding cities. Monitoring the spatial and temporal dynamics of these changes is critical for regulating urban growth, conserving ecologically important land, and promoting environmentally compatible development [6]. Remote sensing provides a consistent and spatially explicit basis for monitoring LULCC across large areas and over extended periods. The increasing availability of multispectral satellite archives, cloud-computing platforms, and machine learning algorithms has substantially improved the capacity to classify land cover and identify long-term environmental change. In particular, GEE provides access to harmonized satellite data and scalable computational resources, while machine learning methods such as RF can accommodate nonlinear relationships among spectral variables and generate accurate land-cover classifications. However, land-cover maps alone do not reveal whether changes in the extent of forests or other natural classes have improved their spatial integrity. Integrating machine learning-based remote-sensing classification with landscape metrics and fragmentation analysis is therefore necessary to connect mapped land-cover transitions with their ecological consequences. Landscape fragmentation is a major outcome of LULCC. It divides continuous habitats into smaller and more isolated patches, alters edge-to-interior relationships, and can reduce biodiversity, ecological connectivity, and ecosystem functioning [7–9]. Quantitative indices such as number of patches (NP), PD, LPI, splitting index, mean nearest-neighbor distance, and contagion (CONTAG) are widely used to characterize the magnitude and spatial distribution of fragmentation [10]. These metrics distinguish changes in landscape composition from changes in spatial configuration. This distinction is important because an increase in total forest area does not necessarily restore structural connectivity when the recovered forest remains dispersed among small, isolated, or poorly connected patches. Urbanization, agricultural intensification, transportation development, and infrastructure expansion are among the principal drivers of landscape transformation and habitat isolation [11,12]. Human activities account for a substantial proportion of observed land-use transitions in many developing regions, emphasizing the need for sustainable land-use planning and conservation strategies [13,14]. Similar pressures are widespread across the Global South, where rapid population growth, economic development, institutional decisions,

deforestation, and unregulated urban expansion have accelerated landscape degradation and fragmentation [15–18]. Fragmentation should therefore be understood not only as a biophysical pattern but also as a socio-ecological outcome of interacting demographic, economic, infrastructural, and policy processes. Green infrastructure, ecological corridors, habitat restoration, and connectivity-oriented land-use planning are increasingly important for maintaining ecological continuity in such landscapes. These challenges are particularly relevant to Islamabad, the capital of Pakistan. The city has experienced rapid population growth, urban expansion, and infrastructure development, resulting in the conversion of forest and agricultural land and increasing pressure on natural habitats [19,20]. Urban growth has also contributed to biodiversity loss, environmental pollution, habitat isolation, and changes in ecosystem functioning. Although reforestation initiatives, including the Billion Tree Tsunami Project, have contributed to increases in forest cover in parts of the region, urban sprawl and transportation development continue to affect landscape integrity [21,22]. Islamabad is therefore an important setting for examining whether gains in forest extent have translated into improvements in forest spatial structure and connectivity. Urban development can support economic production and socioeconomic transformation, but uncontrolled expansion frequently replaces permeable and vegetated surfaces with built-up and impervious land [23–27]. These changes may intensify urban heat, degrade air quality, disrupt hydrological processes, and weaken ecosystem functions [28–30]. In Islamabad, the interaction between urban development, forest restoration, and changing landscape morphology creates a complex environmental trajectory. A spatially integrated assessment is therefore required to evaluate changes in both forest extent and spatial configuration. Previous studies in Pakistan have commonly examined land-cover change, urban growth, or forest-cover trends separately. However, the combined effects of urban expansion and forest recovery on the spatial configuration and structural connectivity of forests in Islamabad remain insufficiently understood. Moreover, relatively few city-scale studies have integrated machine learning-based land-cover classification, multitemporal satellite observations, landscape-pattern metrics, and explicit forest-fragmentation categories within a single analytical framework. Addressing this gap is important for translating remote-sensing observations into information that can support ecological planning and environmental decision-making. This study develops an integrated machine learning and spatial-analysis framework to investigate LULCC and forest fragmentation in Islamabad from 1991 to 2021. Multitemporal Landsat imagery is classified using the RF algorithm in GEE, and the resulting land-cover maps are analyzed using FRAGSTATS 4.3 and the LFT v2.0. Eleven class- and landscape-level metrics—NP, PD, LPI, percentage of landscape (PLAND), landscape shape index (LSI), Euclidean nearest-neighbor distance (ENN), mean patch area (AREA_MN), division index, CONTAG, Shannon's diversity index (SHDI), and Shannon's evenness index (SHEI)—are used to quantify landscape composition, spatial configuration, fragmentation, and structural connectivity. The study specifically aims to: (i) characterize the spatial and temporal patterns of LULCC in Islamabad using machine learning-assisted analysis of multitemporal Landsat imagery; (ii) quantify changes in forest fragmentation and landscape structure using class- and landscape-level metrics in FRAGSTATS and LFT v2.0; and (iii) determine whether recent forest-cover recovery has improved structural connectivity or primarily increased forest extent without restoring landscape integrity. Based on the identified research gap, the study tested the following hypotheses:

H1: *Forest-cover recovery in Islamabad is not necessarily accompanied by a proportional recovery in landscape structural connectivity.*

H2: *Continued urban expansion and agricultural land conversion are associated with increasing forest fragmentation, reflected by greater edge, patch, and perforated forest and reduced dominance of large-core forests.*

H3: *Changes in forest spatial structure may differ substantially from changes in total forest area. By integrating Random Forest-based land-cover classification, multitemporal remote sensing, and landscape-ecological analysis, the study provides spatial evidence that can support forest-fragmentation assessment and inform future urban and landscape planning in Islamabad.*

2. Materials and Methods

2.1. Study Area

The proposed study area is Margalla Hills National Park and Islamabad Capital Territory (ICT) in northern Pakistan, located at approximately (33°14′44.16″ N) and (73°05′04.15″ E) (Figure 1). Islamabad is located on the Potohar Plateau in Punjab Province and serves as the administrative capital of Pakistan. Commercial and industrial activities are concentrated within the planned urban sectors. The territory covers approximately 1010 km^2 and is characterized by mountainous terrain, undulating plains, and elevations ranging from approximately 450 to 600 m. The higher elevations are found primarily in the north, east, and west, while the low-lying areas are found in the south; Margalla Hills National Park is the major physical feature along the northern edge [31]. Islamabad is divided into five main areas (I–V) by the Capital Development Authority (CDA). Zone IV occupies the largest area, and the most developed residential sectors are in Zone I. These include administrative, diplomatic, residential, institutional, industrial, commercial, and rural land uses, green belt, and national park areas [32].

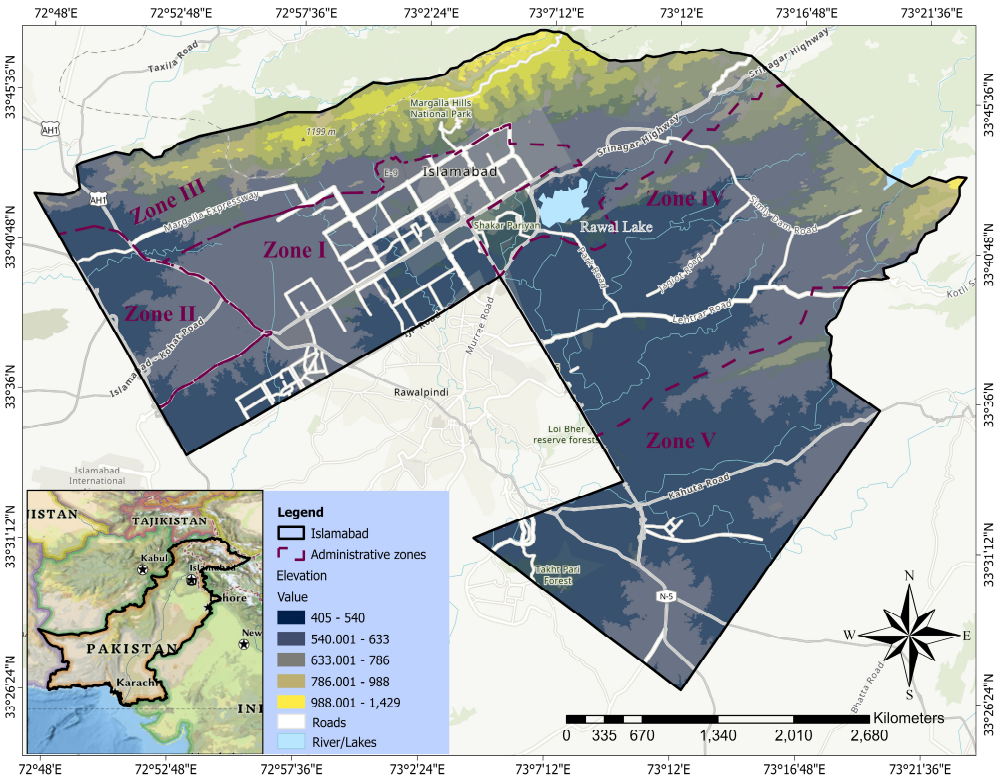


Figure 1. Location map of Islamabad metropolitan area.

Pakistan's 2023 digital census showed that the population of ICT grew from around 2.0 million to around 2.4 million between 2017 and 2023, while urban Islamabad was

estimated at 1.11 million (2023) [33]. This growth has coincided with a rapid expansion of built-up land, increasing by over 341% from 2000 to 2020, primarily due to rising housing demand and infrastructure development [34,35]. Geologically, the area is dominated by Tertiary alluvial deposits, limestone, and sandstone. The region exhibits a humid subtropical climate, characterized by an average yearly temperature of roughly 13 °C. Summers are moderate, whereas winters are generally dry and may occasionally reach freezing conditions.

2.2. Data Sources and Processing

Landscape composition and configuration are aspects that are examined using land-use and land-cover (LULC) maps [36]. In this study, LULC maps were created using the multispectral imagery of Landsat to analyze the LULCC in the city of Islamabad [37]. The multitemporal data (1991–2021) were acquired from Landsat 5 Thematic Mapper (TM), Landsat 7 Enhanced Thematic Mapper Plus (ETM+), and Landsat 8 Operational Land Imager (OLI) and processed in GEE. Images from the study area were selected with reference to ground observations and were cloud-free. The images were classified with a supervised RF algorithm into five different LULC categories: water bodies, forest area, built-up area, bare land, and agricultural area.

The resulting LULC raster maps were imported into FRAGSTATS 4.3 to calculate landscape pattern indices. Spatial variation in landscape structure was further assessed using the moving window method, which enabled the identification of local differences in configuration and fragmentation. Forest fragmentation was analyzed using the LFT to evaluate structural disruption within forested areas. A digital elevation model (DEM) was also used for terrain correction to reduce brightness variations caused by topographic effects.

Landsat Surface Reflectance Tier 1 imagery was used for all classification years. Preprocessing, including calibration, mosaicking, image fusion, clipping, and cloud masking, was performed through the GEE public data catalog. Landsat imagery with 30 m spatial resolution was processed using a median composite approach, in which pixel values from January to December were combined to reduce the influence of seasonal cloud cover. Cloud and cloud-shadow pixels were masked using the QA band following [38]. The cloud-computing capacity of GEE improved the efficiency of image processing [39]. The study area shapefile was uploaded to GEE and used to extract cloud-free Landsat composites for 1991, 2001, 2011, and 2021 [40]. The overall methodological framework adopted in this study, including Landsat data processing, RF classification, landscape metric analysis, and forest-fragmentation assessment, is illustrated in Figure 2.

2.3. Training and Validation

The classification scheme included five dominant LULC classes: water, forest, built-up, bare land, and agriculture. These classes were selected because they represent the mainland cover types associated with urban growth, physiographic variation, and ecological change in Islamabad and can be reliably distinguished using Landsat imagery at 30 m spatial resolution. This classification scheme aids the study goal of evaluating generalized urbanization and forest-fragmentation dynamics. Areas with subclasses that included shrubland, sparse vegetation, and wetlands were classified as forest or vegetation categories using spectral similarity and spatial association with these classes, as done in previous regional LULC classification projects using Landsat data. A 30 m resolution of the Landsat data enables the implementation of an ecologically representative classification scheme with reasonable classification accuracy and is temporally comparable between 1991 and 2021.

Stratified sampling was used to create training and validation samples in GEE from the surface reflectance of Landsat images. This approach ensured spatial representation across

the CDA Zones I-V and along the Margalla–plains gradient. To minimize edge effects and spectral mixing, training samples were manually digitized as small homogeneous polygons located at least one Landsat pixel inside class boundaries. Random validation points were generated at a minimum distance of 100 m from the training polygons for every class and year. QA masks and visual inspection were used to screen all samples for clouds, shadows, and seasonal inconsistencies.

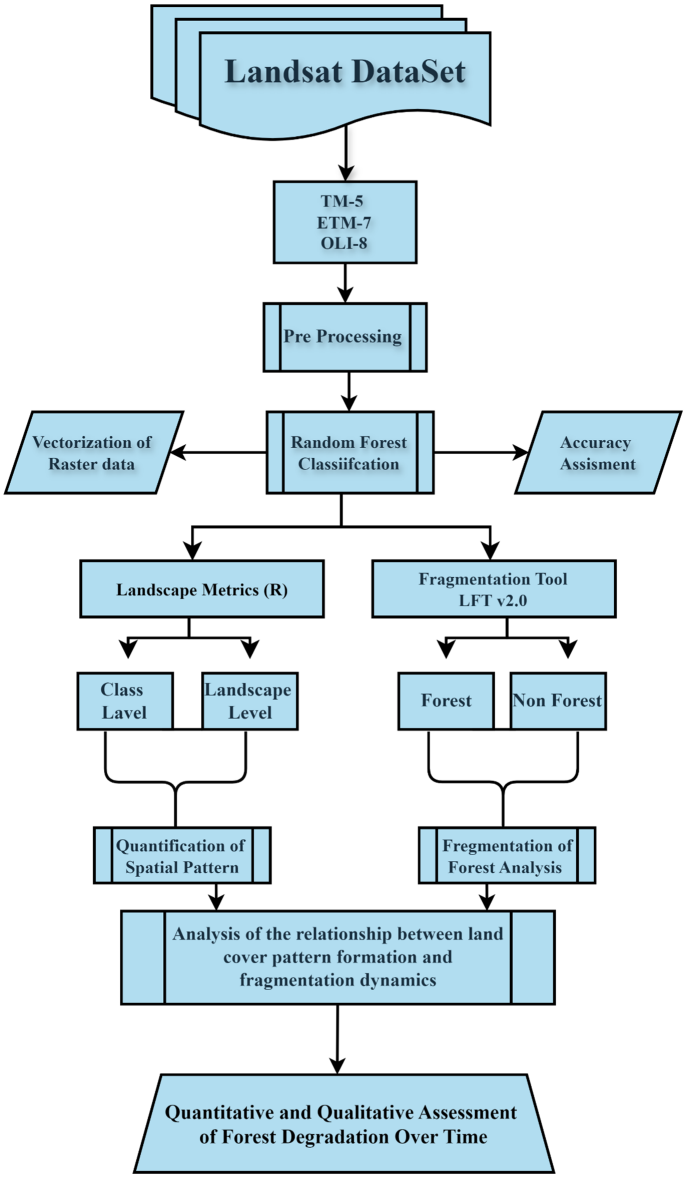


Figure 2. Our Proposed model.

The Sample distribution used for model training and accuracy assessment is presented in Table 1. In total, 70% of the samples were used for training, and 30% were used to assess accuracy. Classification was performed using Landsat Surface Reflectance Tier 1 imagery processed in GEE using the red, green, blue, and near-infrared bands. The accuracy was evaluated using a confusion matrix, and overall accuracy (OA), Kappa coefficient (K), user's accuracy (UA), and producer's accuracy (PA) were computed for each class. For all years, OA was approximately 91%, and the Kappa values were >0.85, which is considered to be a reliable classification.

Table 1. Training and validation sample data.

Years	Training Samples	Testing Samples
1991	1661	504
2001	1473	441
2011	909	272
2021	1027	308

2.4. Land-Use Classification Based on RF

This study uses the RF model, which is frequently applied to land classification. Previous studies [41–45] have shown that RF has achieved higher classification accuracy in LULC studies when compared to Support Vector Machines (SVMs), k-Nearest Neighbors (KNNs), and Maximum Likelihood Classifiers (MLCs). Over the past two decades, its effectiveness in dealing with noisy data and outliers has contributed to its broader use in remote-sensing applications [46,47].

This study adopted RF classification through GEE with three main parameters, i.e., number of trees (Ntree), number of node variables (Mtry), and maximum tree depth (Max Depth). The number of trees was set to 500, while the number of nodes was retained at its default value, corresponding to the total number of input features [48]. OA and K were used to evaluate the accuracy of classification with the help of a confusion matrix. The K was more than 0.8, showing a good classification accuracy criterion [49,50]. The OA for 1991, 2001, 2011, and 2021 was 90.89%, 90.76%, 91.19%, and 91.11%, respectively, with Ks above 0.85, confirming the classification's robustness and reliability.

2.5. LULC Transfer Matrix

The study period was divided into four reference years: 1991, 2001, 2011, and 2021. A transfer matrix was created in ArcGIS 10.5 to quantify LULC transitions between successive periods. The matrix shows the area transformations from land-use classes to other classes, enabling the direction and the amount of change to be determined [51]. The equation gives the transition matrix:

$$A_{ij}\begin{pmatrix} A_{11} & A_{12} & A_{13} & A_{14} & \dots & A_{1n} \\ A_{21} & A_{22} & A_{23} & A_{24} & \dots & A_{2n} \\ A_{31} & A_{32} & A_{33} & A_{34} & \dots & A_{3n} \\ A_{41} & A_{42} & A_{43} & A_{44} & \dots & A_{4n} \\ \dots & \dots & \dots & \dots & \dots & \dots \\ A_{n1} & A_{n2} & A_{n3} & A_{n4} & \dots & A_{nn} \end{pmatrix}$$

where A_{ij} represents the area of land-cover class i at time t that changed to class j at time $t + 1$. For instance, A_{11} denotes the area that remained in class 1, while A_{12} denotes the area that was converted from class 1 to class 2.

2.6. Landscape Pattern Metrics

Landscape metrics were used to quantify the composition and configuration of land-cover patterns derived from remote-sensing data. Landscape pattern metrics are extensively applied in landscape ecology due to their efficient description of patch structure, spatial arrangement, fragmentation, and connectivity [52–54]. Since land-cover change directly alters landscape structure, these indices provide a quantitative basis for assessing spatial transformation over time [55].

Metric selection was based on ecological relevance and the ability of each index to represent structural properties of the landscape. At the class level, NP, LPI, PD, LSI, PLAND, AREA_MN, and ENN were used to measure patch number, fragmentation intensity, dominant patch size, shape complexity, class proportion, AREA_MN, and spatial isolation. At

the landscape level, DIVISION and CONTAG were used to assess landscape subdivision and aggregation, while SHDI and SHEI were applied to measure land-cover diversity and evenness. These metrics together describe the main dimensions of landscape composition, fragmentation, connectivity, and heterogeneity across spatial and temporal scales [52,53,56]. FRAGSTATS 4.3 and RStudio 2026.08.2 were used to calculate the metrics for 1991, 2001, 2011, and 2021 [57]. The formulas and descriptions are provided in Table S1.

2.7. Landscape Pattern Based on Slide Window

The sliding window method was used to examine landscape pattern changes and to capture local variation in fragmentation and heterogeneity at a local scale throughout the study area. This approach identifies spatial differences that may be obscured by whole-landscape statistics [57,58]. The window moves systematically across the raster, and the selected landscape metric is calculated for each window position. The window determines the range of values on which the landscape index is computed [59]. The computed value of the matrix is assigned to the central cell of the window to create a raster map describing spatial distinction in landscape structure [59].

Assessment of landscape fragmentation was conducted using a 3 × 3 pixel moving window corresponding to 300 m. This window size was selected to capture regional-scale spatial heterogeneity and, at the same time, provide enough detail to detect changes in landscape pattern [60].

2.8. Spatio-Temporal Analysis of Forest Fragmentation

Forest fragmentation, characterized by forest loss and spatial pattern changes, is a crucial landscape-level process [61]. Various tools and methodologies have been developed to quantify and analyze forest fragmentation using LULC data [62]. Prominent tools include LecoS Landscape Ecology Statistics (QGIS plugin) [63], FRAGSTAT [56], LFT v2.0 [64], and Morphological Spatial Pattern Analysis (MSPA) [65,66], which are used in this study. The LFT v2.0 tool developed by the Center for Land Use Education and Research (CLEAR) was used to evaluate edge effects and forest fragmentation [67]. It uses morphological image processing for the classification of pixels, which results in a classification of the land as forested or non-forested. LULC was categorized as binary (Table 2) classes of "Forest" and "Non-Forest" and was analyzed with ArcGIS Pro to determine spatial patterns [68]. The edge width parameter of 100 m, a standard threshold in fragmentation analysis, was applied to evaluate the impact of fragmentation on adjacent ecosystems [69]. This threshold reflects the sensitivity of many forest species in subtropical regions and has been widely applied in fragmentation assessments [70]. Although alternative thresholds were not tested here, 100 m provides a balanced estimate of core-area delineation based on prior studies. Forest fragmentation was categorized into six types with four main categories: edge, patch, perforated, and core. The core areas were further subdivided into three size classes: small core (SC) (<1.01 km^2), medium core (MC) (1.01–2.02 km^2), and large core (LC) (>2.02 km^2) (Table 3) [71].

Table 2. Land classes aggregated into forest and non-forest for forest-fragmentation analysis.

No.	Category	Describe	Reclassified LC
1	Water	Areas covered by water.	Non-Forest
2	Forest	Areas covered by forest.	Forest
3	Built-up	Land modified by human infrastructure.	Non-Forest
4	Bare land	Includes all bare land types, such as rocky, agricultural, and urban bare land	Non-Forest
5	Agriculture	Agricultural land.	Non-Forest

Table 3. Components of forest fragmentation and their ecological definitions.

Fragmentation Components	Ecological Definition
Patch	A discrete, isolated area of forest resulting from the fragmentation of a larger continuous forest.
Perforation	Small gaps or openings within a forest are caused by non-forest elements like roads or agricultural fields.
Edge	The forest and non-forest areas are often characterized by changes in environmental conditions and species composition.
Core	The interior area of a forest patch, undisturbed by edge effects, is critical for biodiversity and ecosystem stability.

To quantify temporal changes in individual forest-fragmentation classes, the area change in each class between two consecutive years was calculated as:

$$\Delta A_i = A_{i,t_2} - A_{i,t_1}$$

where ΔA_i is the area change (km^2) of fragmentation class i, and A_{i,t_2} and A_{i,t_1} are the areas of that class at the beginning and end of the corresponding period, respectively. The contribution of each fragmentation class to the net change in total forest area was then calculated as:

$$C_i = \frac{\Delta A_i}{\Delta A_F} \times 100$$

where C_i is the contribution of fragmentation class i to the net forest-area change (%) and ΔA_F is the net change in total forest area, calculated as:

$$\Delta A_F = F_{t_2} - F_{t_1}$$

Because gains and losses among individual fragmentation classes may offset one another, the absolute value of C_i may exceed 100%. Positive or negative values indicate whether the change in a fragmentation class occurred in the same or opposite direction as the corresponding net change in total forest area.

3. Simulation and Results

The results of LULC classification, landscape metrics analysis, and forest-fragmentation assessment are presented for Islamabad for the period 1991–2021 in this section. The results show the spatial and temporal variations derived from multitemporal Landsat imagery classified using the RF algorithm in GEE. Landscape composition, configuration, and connectivity change were quantified using FRAGSTATS and LFT outputs. The results are given in four sections: (i) analysis of the distribution of LULC over four time periods, (ii) assessment of the landscape-level metrics, (iii) spatial pattern of fragmentation, and (iv) the key findings that identify the change and their ecological implications.

3.1. Land-Use and Land Cover Changes (1991–2021)

The built-up areas have increased significantly in Islamabad from 1991 to 2021, while the agricultural area has decreased and forest cover has changed. Agricultural land decreased from 49.22% of the study area in 1991 to 25.82% in 2021. In the same period, there was also an increase in the built-up area from 76 km^2 (7.5%) to 259 km^2 (25.6%), continuing the trend of land being converted from non-urban to built-up during the last twenty years. Forest cover increased from 322.25 km^2 in 1991 to 340.86 km^2 in 2001, declined to 271.96 km^2 in 2011, and subsequently increased to 409.22 km^2 in 2021. This pattern reflects alternating

periods of forest gain and loss over the study period. The bare land experienced smaller changes; bare land increased during the earlier decades, followed by a decrease in 2021, and water bodies were relatively stable throughout the study, not exceeding 1% of the total area. Table 4 shows the area and percentage of each LULC class, and Figure 3 displays the spatial distribution of each LULC class.

Table 4. LULC of the study area in 1991, 2001, 2011, and 2021.

LULC	Area (km^2)	%	Area (km^2)	%	Area (km^2)	%	Area (km^2)	%
Year	**1991**		**2001**		**2011**		**2021**	
Water	7.93	0.79	9.02	0.89	6.03	0.6	7.91	0.78
Forest	322.25	31.9	340.86	33.74	271.96	26.92	409.22	40.5
Built-up	76.31	7.55	129.33	12.8	217.85	21.56	258.62	25.6
Bareland	106.53	10.54	111.75	11.06	139.54	13.81	73.67	7.29
Agriculture	497.22	49.22	419.29	41.5	374.85	37.11	260.83	25.82

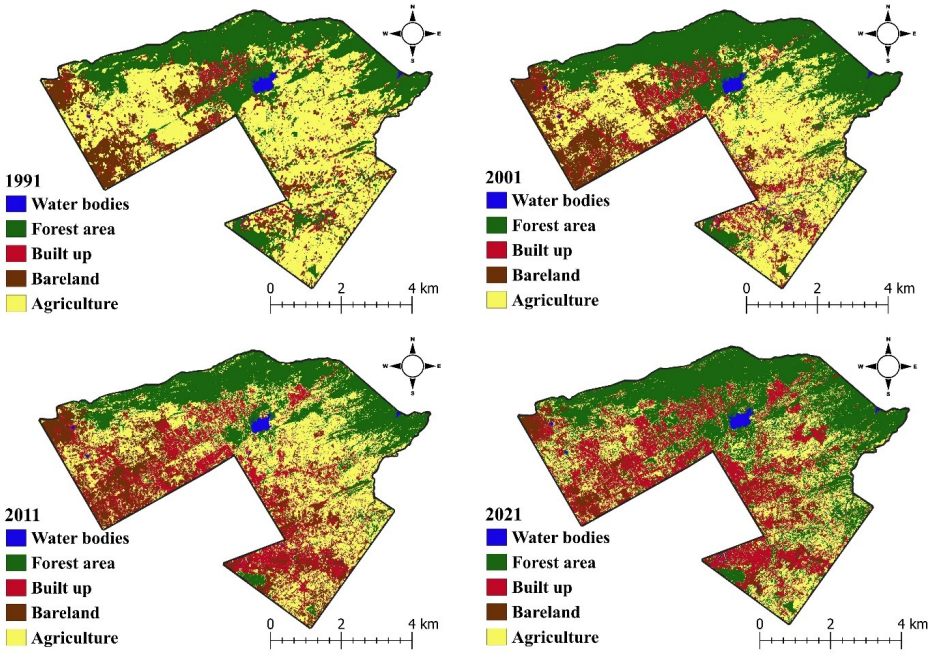


Figure 3. LULC map for the years 1991, 2001, 2011, and 2021.

Built-up expansion was the most prominent observed LULC transition, particularly involving the conversion of agricultural and other non-urban land. Forest cover showed alternating periods of decline and increase, occurring alongside continued land-use change and reported conservation activities in the region. The changes suggest land-use planning that restricts unplanned urban growth and promotes actions for reforestation and sustainable landscape management. In addition to absolute area change (km^2), the percentage contribution of each LULC class to the total absolute land-cover change within each period was calculated to facilitate comparison among classes (Table 5).

Table 5. LULCC in the metropolitan area during 1991–2001, 2001–2011, 2011–2021, and 1991–2021.

LULC % Classes	Change 1991–2001	% Absolute Change	Change Between 2001 and 2011	Change in Absolute %	Change Between 2011–2021	Change in Absolute %	Change Between 1991 and 2021	Change in Absolute %
Water	+1.09	0.70	−2.99	1.29	+1.88	0.52	−0.03	0.01
Forest	+18.61	11.94	−68.90	29.61	+137.25	38.15	+86.97	16.15
Built-up	+53.02	34.02	+88.53	38.05	+40.76	11.33	+182.31	33.85

Table 5. *Cont.*

LULC % Classes	Change 1991–2001	% Absolute Change	Change Between 2001 and 2011	Change in Absolute %	Change Between 2011–2021	Change in Absolute %	Change Between 1991 and 2021	Change in Absolute %
Bareland	+5.22	3.35	+27.80	11.95	−65.88	18.31	−32.86	6.10
Agriculture	−77.93	50.00	−44.44	19.10	−114.02	31.69	−236.39	43.89

Note: "+" indicates increased area, "−" indicates decreased area (km^2). Note: "Change" indicates an area increase or decrease in km^2. The % absolute change represents the contribution of each LULC class to the total absolute land-cover change during the corresponding period.

Transformation of Different LULC Classes

The land-use transition analysis (Figure 4; Table S2) makes it clear which are the most important conversion pathways that underlie the observed LULC changes. During the 30 years, the agricultural class was primarily replaced by the built-up and forest classes, with an approximate conversion of 142.4 km^2 to built-up and 125.3 km^2 to forest. These transitions show that substantial portions of agricultural land were converted to built-up and forest classes, contributing directly to the observed decline in agricultural area and increase in mapped forest cover. During 1991–2001, agricultural conversion remained relatively limited, with about 5.5% of farmland changing to forest and 4.6% to built-up land, showing early transitions from agricultural land to forest and built-up classes (Table S2). Between 2001 and 2011, urban expansion accelerated, as 8.7% of agricultural land was converted to built-up areas, while forest area declined by 6.2%. In 2011–2021, this pattern partly shifted, with 13.0% of farmland converted to forest cover, contributing to the recovery of forest area, while 5.7% of bare land changed to built-up use as urban development continued. These transition patterns are consistent with the net area changes and identify agricultural-to-built-up and agricultural-to-forest conversions as important components of Islamabad's observed landscape transformation.

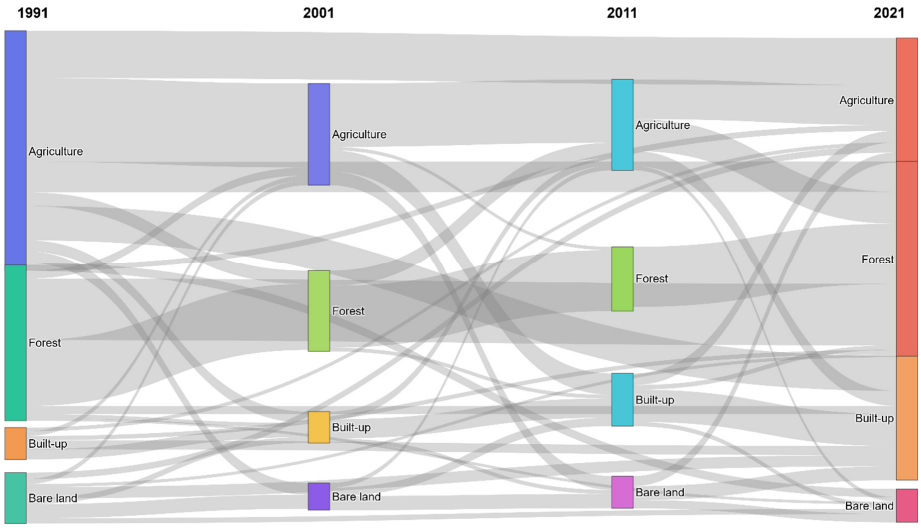


Figure 4. Major land-use and land-cover transition pathways in Islamabad during the study period. For visual clarity, unchanged land-cover areas and transitions representing less than 1% of the study area are not displayed; the complete transition matrix is provided in Table S2.

The period-by-period percentage changes in Figure 5 show continued built-up expansion, declining agricultural land, and variable forest cover. Urban area increased in each interval, while cropland decreased, with the largest changes occurring during 2001–2011. On the other hand, forest cover decreased during the same time period and has increased since 2011, due to forest loss and later restoration. The patterns are in line with the re-

sults of the transfer matrix and suggest a trade-off between increasing built-up cover and decreasing natural and agricultural cover. The patterns of forest losses and subsequent recovery observed during the study period need to be further investigated; this is why Section 3.2 investigates the patterns of forest loss and recovery at the spatial level during the study period.

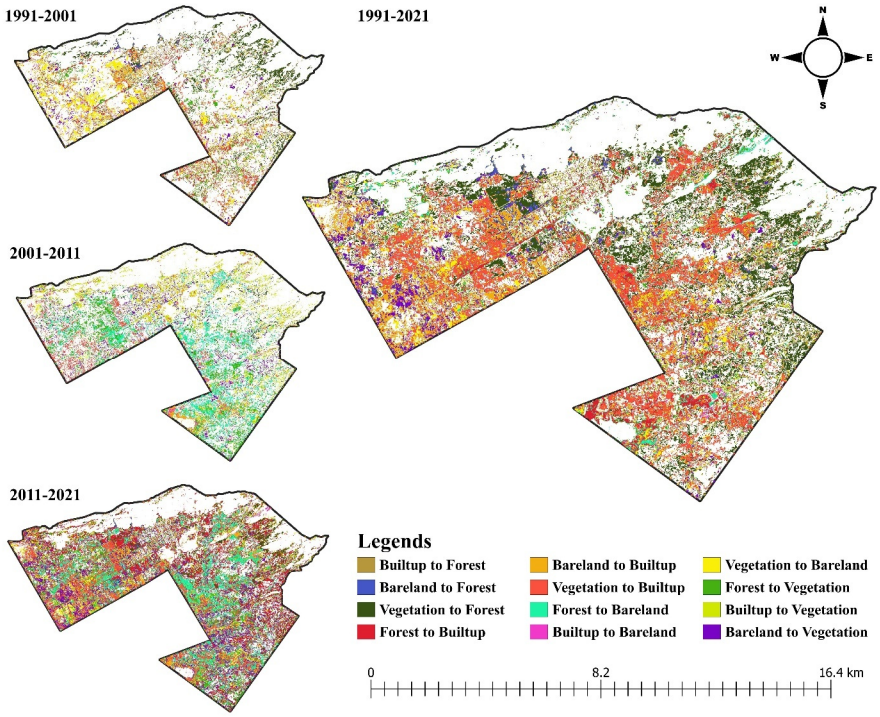


Figure 5. LULC variations in Islamabad from 1991 to 2021.

The urban area continues to expand, and forest cover is being lost and gained to varying extents, while agricultural land is on a downward trajectory as shown in Figure 5. They also highlight the need for city planning that will help to stop the conversion of farmland and promote reforestation and sustainable management of the landscape. Forest gain/loss and spatial distribution are explored further below for the study period (Figure 6).

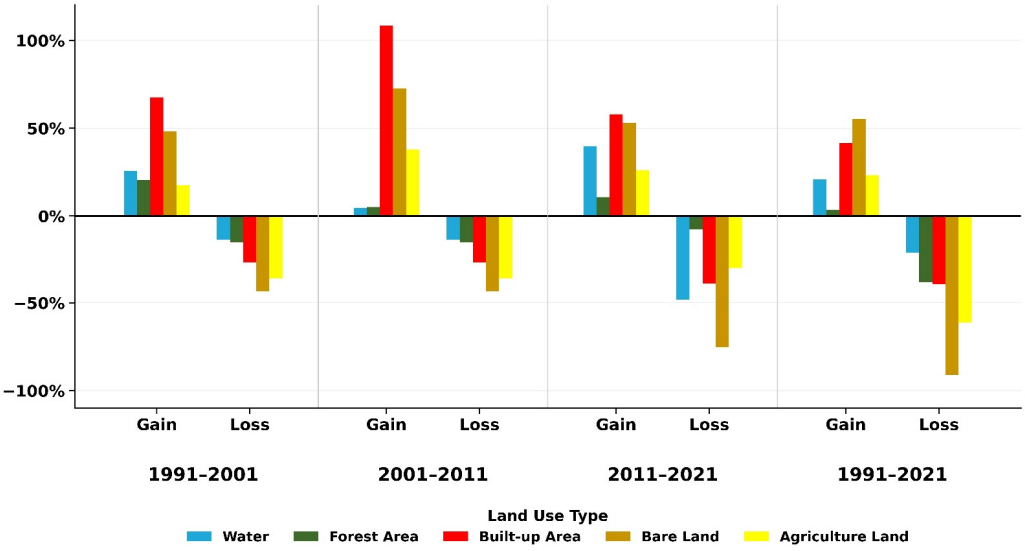


Figure 6. Percentage variation in land-use types in metropolitan areas over different time periods (1991–2001, 2001–2011, 2011–2021, and 1991–2021).

3.2. Forest Cover Dynamics and Spatial Distribution (1991–2021)

Forest cover in Islamabad and the surrounding Margalla Hills changed considerably between 1991 and 2021, subject to a variety of factors, including deforestation, encroaching urban development, and reforestation. The northern areas showed mostly recovery due to conservation and plantation activities, such as the Billion Tree Tsunami Project, which led to an increase in forest cover. Forest loss was more evident in the central and southern parts of Islamabad, where urban expansion continued to exert pressure on forested land (Figure 7). Forest cover increased during 1991–2001, declined between 2001 and 2011, and recovered during 2011–2021 due to afforestation and protection measures taken in Margalla Hills National Park (Table 6; Figure S2). In this analysis, 'loss' refers to forest areas converted to non-forest classes, whereas 'gain' refers to areas converted from non-forest classes to forest. Losses were mostly concentrated in the expanding urban fringe, while forest regeneration was mostly concentrated in protected areas. These changes indicate forest recovery in the face of persistent urban pressures, highlighting the need for conservation planning and managed urban development in order to build landscape resiliency.

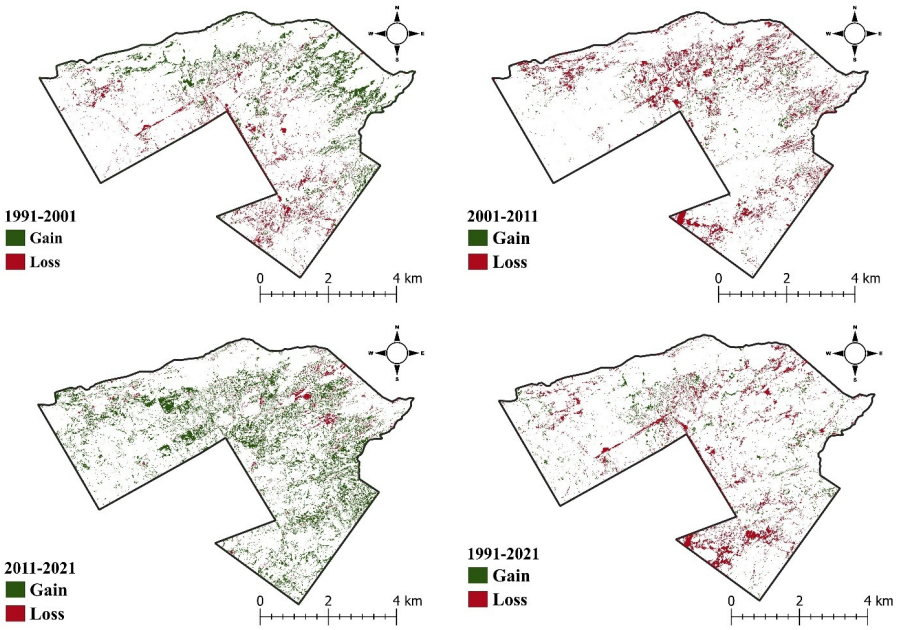


Figure 7. The Forest gain and loss map classification for Islamabad, 1991–2021.

Table 6. Forest area and temporal changes in total forest cover for each period (1991–2021).

Years	Initial Forest Area (km^2)	Final Forest Area (km^2)	Forest Loss (km^2)	Forest Gain (km^2)
1991–2001	322.25	340.85		18.61
2001–2011	340.85	271.96	68.89	-
2011–2021	271.96	409.22	-	137.25

3.3. Forest-Fragmentation Analysis

The spatial distribution of forest fragmentation changed considerably between 1991 and 2021, indicating substantial changes in forest structural configuration (Figure 8). Using the 100 m edge threshold, forest areas were categorized as edge, patch, perforated, small-core (SC), medium-core (MC), and large-core (LC).

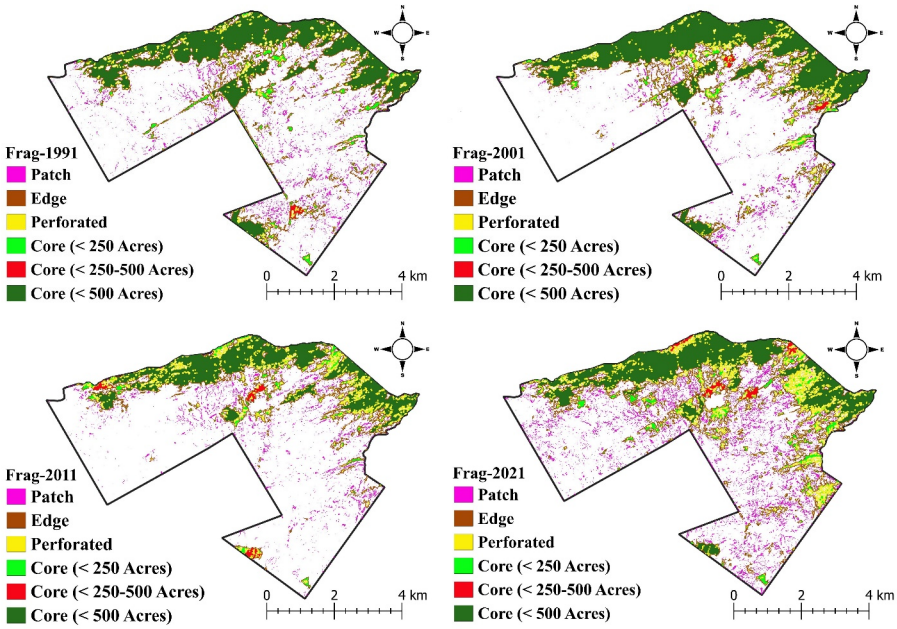


Figure 8. Forest-fragmentation patterns in Islamabad (1991–2001, 2011–2021).

In 2001, large-core (LC) forests represented 57.99% of the total forest area, but its proportion declined to 35.56% by 2021, indicating a reduction in the relative dominance of large-core forests. In absolute terms, large-core forests decreased from 197.68 km^2 in 2001 to 145.50 km^2 in 2021. Patch forests increased from 1.39 km^2 (0.43%) in 1991 to 72.93 km^2 (17.82%) in 2021, indicating a substantial increase in isolated forest fragments (Figure 9). Perforated forests increased from 25.92 km^2 (8.04%) in 1991 to 75.58 km^2 (18.47%) in 2021, indicating a substantial expansion of internally fragmented forest areas. Small-core forests increased from 10.22 km^2 in 2011 to 18.39 km^2 in 2021. These fragmentation changes occurred alongside substantial built-up expansion and agricultural land conversion documented by the LULC analysis. The increase in patch and perforated forests, together with the reduced relative dominance of large-core forests, indicates a shift toward greater structural fragmentation and reduced forest continuity in Islamabad. A sensitivity analysis was conducted for the 2021 forest map using edge thresholds of 50, 100, and 150 m (Table S5). Although the estimated proportions of individual fragmentation classes varied with edge distance, the overall interpretation of substantial forest fragmentation remained consistent. Large-core forests accounted for 49.31% of total forest area at the 50 m threshold, compared with 35.56% at 100 m and 29.95% at 150 m. Conversely, the combined proportion of patch and perforated forests increased from 13.56% at 50 m to 36.29% at 100 m and 46.01% at 150 m. These results demonstrate that the absolute extent of individual fragmentation classes is threshold-sensitive, particularly for core forests, while the presence of considerable structural fragmentation is evident across all three tested thresholds.

Transitions and Change Matrices of Forest Fragmentation

Changes in the spatial pattern of forest fragmentation from 1991 to 2021 indicated changes in landscape connectivity (Figure 8). Forest areas were classified into six categories—patch, edge, perforated, SC, MC, and LC. Each category represents a different ecological condition. LC areas encompass relatively undisturbed interior forest habitats that provide for biodiversity and ecological stability. SC and MC forests contain interior habitats but are more susceptible to edge effects than large-core forests. Perforated forests are forests that have internal openings within a forest block, which may be associated with human disturbance, and habitat quality may be declining, while patch forests are isolated frag-

ments that generally provide limited habitat connectivity and ecological function. Forest structure and connectivity have changed over the study period (Figure 10; Tables 7 and S4). Edge-to-edge transitions remained high, with values of 7.85 during 1991–2001 and 7.12 during 2011–2021. Patch-to-patch persistence increased from 2.37% during 1991–2001 to 3.47% over the full 1991–2021 period, indicating persistence and expansion of isolated forest patches. The degradation was highest in the LC forest class between 2001 and 2011, with a rise in LC-to-perforated transitions to 14.97, indicating fragmentation of once-continuous patches of forest.

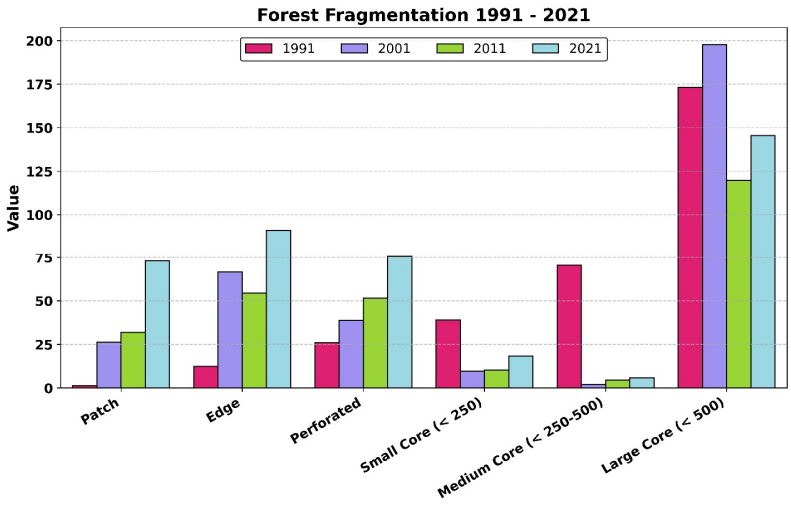


Figure 9. Forest-fragmentation trend from 1991–2021.

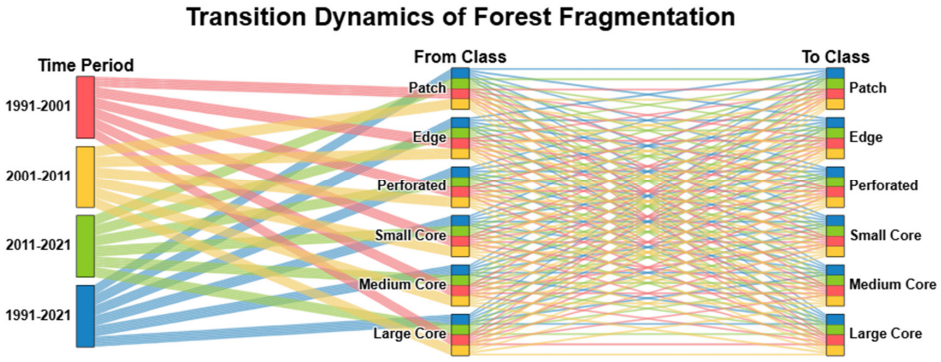


Figure 10. Transitions across forest fragmentation (1991–2021).

SC and MC forests did not have as major a role, and the MC class represented only 5.80 km^2 (1.42%) of forest area in 2021. Perforated forests increased in size over time and were more highly fragmented in 2011–2021 (8.62) than in 1991–2001 (2.28), indicating increasing persistence of internally fragmented forest areas. Over the entire study period, LC areas shifted to edge (3.81) and perforated (7.50) classes, and there was only partial regeneration from perforated areas to larger core forest areas.

These transitions show a sequence of early edge formation and patch development during 1991–2001, rapid fragmentation and core loss during 2001–2011, and continued edge dominance with localized regeneration during 2011–2021. Patch forests increased from 0.43% to 17.82%, perforated forests from 8.04% to 18.47%, and edge forests from 3.84% to 22.24%, whereas the proportion of large-core forests declined from 53.72% to 35.56%. These patterns suggest that urban expansion, agricultural encroachment, and infrastructure development have progressively fragmented Islamabad's forests. The following section examines landscape- and class-level metrics further to quantify these spatial changes across

all land-cover classes and to assess how urban expansion and land-use transitions have altered Islamabad's ecological structure.

Table 7. Temporal changes in forest-fragmentation classes and forest/non-forest cover in Islamabad from 1991 to 2021. The periods (a), (b), and (c) represent 1991–2001, 2001–2011, and 2011–2021, respectively. Change (km^2) represents the difference in area of each fragmentation class between consecutive years, while contribution to net forest-area change (%) represents the area change in each fragmentation class relative to the corresponding net change in total forest area. Values may exceed ±100% because gains and losses among individual fragmentation classes can offset one another.

Classes	1991 km^2	%	2001 km^2	%	2011 km^2	%	2021 km^2	%	Change (a)	%	Change (b)	%	Change (c)	%
Patch	1.39	0.43	26.19	7.68	31.87	11.72	72.93	17.82	24.8	1784.17	5.68	21.69	41.06	128.84
Edge	12.39	3.84	66.46	19.5	54.32	19.97	91.01	22.24	54.07	436.40	−12.13	−18.27	36.68	67.54
Perforated	25.92	8.04	38.85	11.4	51.45	18.92	75.58	18.47	12.93	49.88	12.61	32.43	24.13	46.90
SC	38.94	12.08	9.57	2.81	10.22	3.76	18.39	4.49	−29.38	−75.42	0.65	6.79	8.17	79.94
MC	70.5	21.88	2.12	0.62	4.5	1.65	5.8	1.42	−68.37	−96.99	2.37	112.26	1.3	28.89
LC	173.1	53.72	197.68	57.99	119.61	43.98	145.5	35.56	24.56	14.20	−78.07	−39.49	25.91	21.65
Forest	322.2	31.9	340.86	33.74	271.96	26.92	409.2	40.51						
N-Forest	687.9	68.1	669.39	66.26	738.28	73.08	601	59.49						

3.4. Landscape-Level and Class-Level Metrics and Their Link to Land-Use Drivers (1991–2021)

3.4.1. Landscape-Level Changes

The spatiotemporal analysis of landscape patterns from 1991 to 2021 showed structural changes across the five LULC categories, measured using landscape- and class-level indices. Seven class-level metrics—NP, PD, LPI, PLAND, LSI, ENN, and AREA_MN—were used to assess changes in landscape structure and fragmentation intensity (Figure 11).

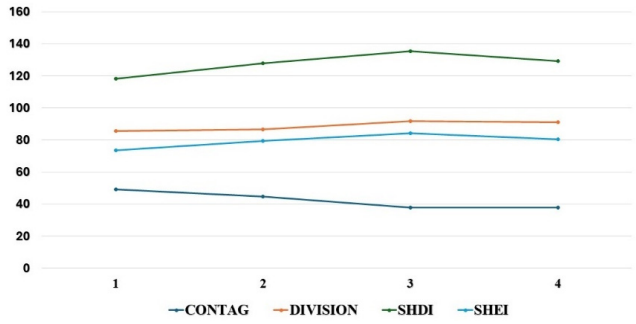


Figure 11. Temporal trends in landscape metrics in Islamabad (1991–2021).

At the landscape scale, CONTAG decreased from 49.22 in 1991 to 37.99 in 2011, indicating the fragmentation of previously continuous land-cover mosaics associated with the expansion of roads, housing, and mixed land uses. During the same period, DIVISION increased from 0.85 to 0.91, reflecting greater subdivision into smaller and more isolated patches. Both indices stabilized after 2011, indicating a slower rate of additional subdivision after 2011. SHDI increased from 1.18 in 1991 to 1.36 in 2011, while SHEI increased from 0.73 to 0.84, indicating greater land-cover diversity and a more even distribution of land-cover classes. The changes indicate that fragmentation intensified until 2011 and became less pronounced thereafter.

Classes of forest fragmentation are patch, perforated, transitional, SC, and LC, which represent different ecological conditions. Patch forests are isolated forest fragments that generally provide limited habitat connectivity. Perforated forests contain openings created because of internal disturbance. Transitional zones are areas of disturbance and/or

regrowth; SC forests provide limited interior habitat, and LC forests are more stable, with core forest conditions. A 100 m edge width was used to define these classes, as this is the approximate depth of edge influence of microclimate and biota found in regional forest edge studies.

3.4.2. Class Level Dynamics

At the class level, substantial structural changes were observed in forest, agricultural, built-up, bare land, and water classes between 1991 and 2021. These changes are generally related to urban expansion, agricultural decline, and local forest regeneration. Built-up area increased from 7.55% in 1991 to 21.56% in 2011, while agricultural land decreased from 49.22% to 37.11%. Forest cover increased in 2001, declined by 2011, and recovered by 2021. The class-level metrics (Table S3 and Figure 11) are derived based on these LULC changes.

NP and PD increased in built-up and agricultural classes, indicating a greater number of smaller patches than in any other class (Figure 12). NP increased substantially in the built-up class, from 5566 in 1991 to 9211 in 2011, indicating greater spatial subdivision of built-up patches during this period. The forest NP in 1991 was 5650, then reduced to 2868 in 2001, and increased to 3787 in 2011, indicating a loss and a partial recovery due to replanting and conservation. There were also increases in NP and PD in barren areas after 2001, potentially associated with the removal of vegetation cover and disturbance of the surface associated with construction and erosion processes.

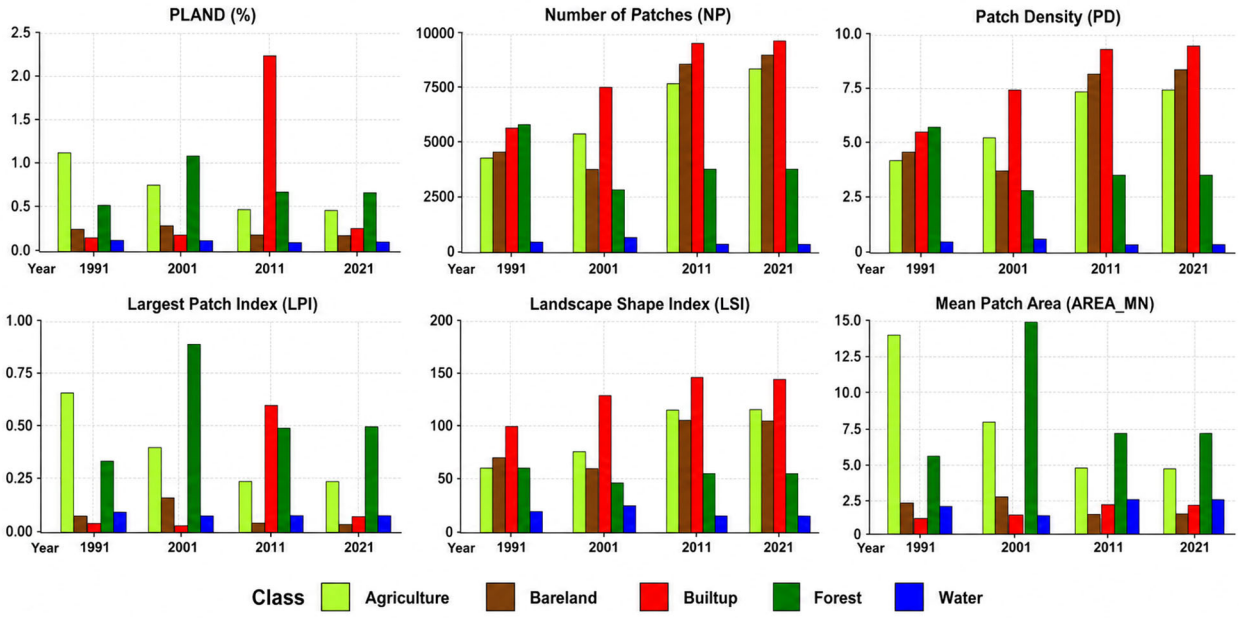


Figure 12. Class-level metrics of LC patterns (1991–2021).

The differences in the dominance and continuity of land-cover classes were apparent in LPI values. The decline of the agricultural LPI from 29.26% in 1991 to 2.99% in 2021 was due to the fragmentation of large farmland blocks. The proportion of built-up LPI increased from 0.68% to 7.23%, indicating the consolidation of previously dispersed settlements into larger urban clusters. Forest LPI was at 26.90% in 2001, dropped in 2011, and rose in 2021 to 27.96%, similar to forest loss and regrowth. The area of continuous bare land surfaces decreased from 5.86% in 2001 to 0.62% in 2021 (bare land LPI), representing a decrease in the amount of continuous bare land surfaces and indicating greater fragmentation of previously continuous barren surfaces.

Additional values of ENN characterize the isolation of classes. Forest ENN increased up to 2001, indicating greater separation among forest patches, and subsequently declined

by 2021, indicating reduced mean nearest-neighbor distance among forest patches. ENN in built-up areas declined gradually, suggesting denser urban development and shorter distances between urban patches. Agricultural ENN also decreased, indicating a tendency to cluster towards urban extremities. The averages in AREA_MN showed similar trends: average patch size increased in urban areas, agricultural and bare land classes became more fragmented, and forest patches moderately recovered after 2011.

3.4.3. Spatial and Temporal Variations in Fragmentation and Diversity

The landscape fragmentation and landscape heterogeneity in Islamabad have been increasing over the years, as shown in the landscape metrics for 1991–2021 (Figures 13 and 14). PD maps indicate that fragmentation expanded from localized mixed-use areas to broader parts of the metropolitan landscape. The high PD values were predominantly found in areas with agricultural use and natural vegetation, whereas the northern and peripheral areas still had low fragmentation in 1991.

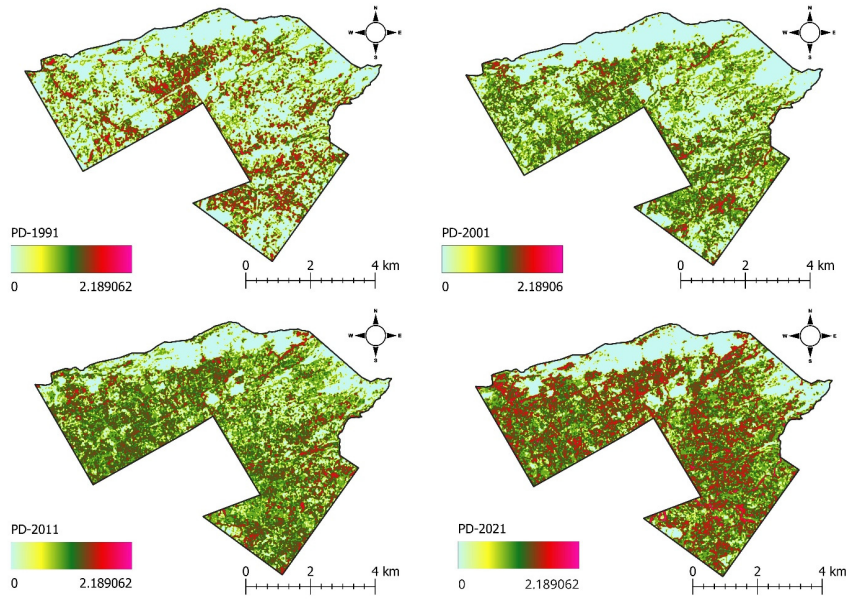


Figure 13. Spatial distribution of PD in the study area from 1991 to 2021.

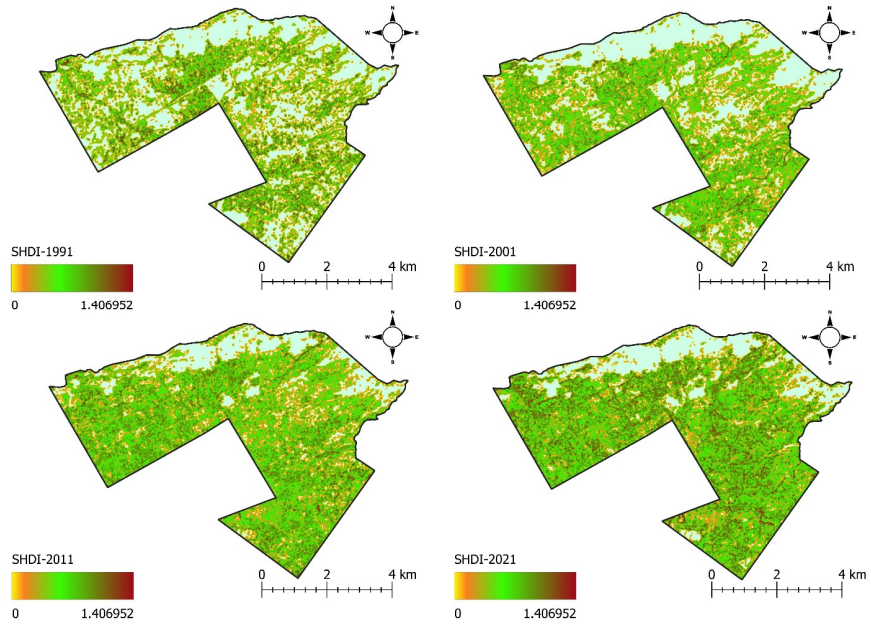


Figure 14. Spatial distribution of SHDI from 1991 to 2021.

By 2001, higher fragmentation had extended into transitional areas and spatially coincided with areas undergoing substantial land-cover conversion. Compared to 2011, high-PD clusters became concentrated around the metropolitan core, suggesting fragmentation of larger habitat patches and a decrease in ecological connectivity in the 2011–2021 period.

3.4.4. Spatial Patterns of Landscape Diversity (SHDI)

SHDI patterns also indicate increasing land-cover heterogeneity. High SHDI values were found in mixed agricultural/vegetated areas, where more diversity in land cover existed but was limited in space in 1991. Over time, the SHDI values increased in central, north, and eastern Islamabad, which aligned with changes in the use of agricultural land and urban expansion (Figure 14). In 2021, greater diversity in land-use mosaics around the urban core was becoming more prominent, while low SHDI values were primarily located in forest highlands with little human use. The increase in both PD and SHDI indicates that the landscape became more fragmented and compositionally diverse over time, alongside substantial changes in built-up, agricultural, and forest land cover.

3.5. Summary of Key Findings

Islamabad has experienced a transition from agriculture to urbanization from 1991 to 2021. The built-up area grew from 7.55% to 25.6%, and the agricultural area shrank from 49.2% to 25.8%. The forest cover has been shrinking in the 2001–2011 period, followed by an expansion after 2011, partly due to conservation and plantation programs like the Billion Tree Tsunami Project. Integrated analysis of LULC transitions, landscape metrics, and forest-fragmentation classes reveals that forest recovery was not always accompanied by increased connectivity. Edge, patch, and perforated classes increased in size, and large-core forests were further subdivided. An increase in PD and DIVISION and a decrease in CONTAG means that there is increased spatial subdivision and decreased landscape aggregation.

4. Discussion

The present study assessed LULC change and forest fragmentation in Islamabad from 1991 to 2021, based on remote-sensing data and landscape metrics. This period saw an increase in built-up area and a decrease in agricultural land due to conversion to urban uses, especially since 2001 [72]. Forest cover increased from 1991 to 2001, decreased during 2001–2011, and then partially recovered during 2011–2021, partly due to reforestation efforts like the Billion Tree Tsunami Afforestation Project (BTTAP) [73]. The increase in forest area, however, did not match full forest structural recovery. PD increased, and CONTAG declined, indicating greater subdivision and lower aggregation of forest patches. Further evidence of fragmentation of previously continuous core forest areas is provided by the decline of forest LPI during the main disturbance period [74].

These results provide support for the proposed hypotheses. H1 was supported because forest-cover recovery after 2011 was not accompanied by a proportional recovery in forest structural connectivity, as reflected by the reduced dominance of large-core forest and increased patch, edge, and perforated classes. H2 was supported at the level of spatial association, as built-up expansion and agricultural land conversion occurred alongside increased landscape fragmentation and reduced aggregation; however, causality was not directly tested. H3 was supported because landscape-configuration metrics and forest-fragmentation classes consistently showed that changes in forest spatial structure differed from changes in total forest area.

The LULC and fragmentation patterns of Islamabad are echoed by similar patterns reported by other rapidly growing cities in Asia. Urbanization has led to widespread loss of agricultural and forest land in cities, creating more discontinuous landscapes and decreas-

ing ecosystem functions in cities including Mumbai, Dhaka, Colombo, and Tokyo [75–78]. These processes have also been reported in two other regions: the Yangtze River Basin in China, where natural and agricultural land has been converted to built-up areas, leading to decreased habitat connectivity, and Khyber Pakhtunkhwa, Pakistan, where population growth and economic development have contributed to the loss of natural and agricultural habitats [79–81]. The conversion of cropland and forest land also led to the decline of ecosystem services and increased landscape fragmentation in the major grain-producing areas in China [82,83]. Research from Nanjing, China, and Athens, Greece, also shows that afforestation and green infrastructure, if not combined with ecological connectivity measures, may not compensate for the impacts of ongoing urban sprawl [84,85].

The outcomes are consistent with one of the key tenets of landscape ecology, that urban development can fragment habitats, increase edge effects, and decrease the functional continuity of natural systems [86]. Fragmentation seems to be as significant as forest loss in Islamabad. The forest-cover has been recovered in several areas since 2011 due to BTTAP and other plantation projects. However, many forest areas are still physically fragmented, and stands are small and interspersed with other land uses. This is important because not all forest cover growth necessarily enhances habitat connectivity or ecological function. These findings suggest that future restoration planning could benefit from considering the spatial arrangement of forest patches, conservation of core habitats, and measures to limit further fragmentation associated with urban expansion. Green infrastructure, urban forests, and greenbelts may contribute to reducing habitat isolation and supporting ecosystem services such as carbon sequestration, microclimate regulation, and water management, although these functions were not directly evaluated in the present study [79].

The following limitations should be considered when interpreting the results. First, the 30 m spatial resolution of Landsat may underrepresent small forest patches, narrow ecological corridors, fragmented urban green spaces, and fine-scale land-cover transitions, particularly within heterogeneous urban–forest interfaces. Consequently, some local fragmentation patterns may not be fully captured, and future studies could use higher-resolution data such as Sentinel-2 or commercial satellite imagery to evaluate these features in greater detail. Second, the landscape metrics and LFT-derived fragmentation classes used in this study quantify structural characteristics of the landscape but do not directly measure functional connectivity or ecological processes such as species movement, habitat use, microclimatic responses, or population dynamics. Therefore, reduced structural connectivity should not automatically be interpreted as an equivalent reduction in functional connectivity for all species. Integrating field observations, biodiversity indicators, species-specific movement data, and habitat-quality assessments would provide a more comprehensive evaluation of the ecological consequences of fragmentation. Third, socioeconomic and policy-related factors, including population growth, infrastructure expansion, urban planning decisions, and restoration programs, were not explicitly incorporated into the spatial models. Their inclusion in future analyses would help distinguish observed land-cover associations from the underlying processes contributing to landscape change.

In addition, although the land-cover classifications achieved overall accuracies of approximately 91% with Kappa coefficients above 0.85, classification uncertainty may propagate into the derived fragmentation metrics. In particular, isolated misclassified pixels or small clusters can artificially increase the number of patches and patch density, especially in heterogeneous urban–forest transition zones. Therefore, the absolute magnitudes of NP and PD should be interpreted with some caution. However, the fragmentation interpretation in this study is based on multiple complementary indicators, including PD, LPI, CONTAG, DIVISION, forest-fragmentation classes, and their multitemporal spatial patterns, rather than on patch density alone. Future studies could explicitly propagate classification un-

certainty into landscape metrics through repeated classifications, error-adjusted maps, or sensitivity analyses using higher-resolution imagery.

Despite these limitations, the results highlight the importance of considering forest spatial configuration alongside total forest-cover change in rapidly urbanizing landscapes. For Islamabad, the findings suggest that future restoration and land-use planning could benefit from protecting existing core forests, improving the spatial continuity of restored forest patches, and considering connectivity when evaluating reforestation outcomes. Future research should integrate socioeconomic and policy-related variables, including population growth, infrastructure development, urban-planning decisions, and restoration initiatives, to better explain the processes associated with observed LULC and fragmentation patterns. Higher-resolution and more frequent remote-sensing observations, together with biodiversity, habitat-quality, and species-movement data, would also help distinguish structural connectivity from functional ecological connectivity. Applying the integrated LULC–landscape metric–fragmentation framework to other rapidly urbanizing regions could provide comparative evidence on whether increases in forest cover consistently translate into improvements in landscape structure and could support more spatially informed urban restoration and conservation planning.

5. Conclusions

This study quantified LULCC and forest-fragmentation dynamics in Islamabad between 1991 and 2021 using multitemporal remote sensing, RF classification, and landscape-pattern analysis. The findings show that rapid urban expansion and the reduction in agricultural land were associated with greater habitat fragmentation and declining landscape structural connectivity. Although reforestation initiatives, including the BTTAP, contributed to the recovery of forest cover, the fragmentation metrics indicate that this increase in forest area did not produce a corresponding restoration of forest structural integrity. High PD, together with low CONTAG and a reduced LPI, revealed the continued subdivision and limited aggregation of forest patches. Although forest cover increased substantially after 2011, fragmentation metrics indicated persistent spatial subdivision and limited aggregation of forest patches. The findings suggest that sustainable land management in Islamabad should consider landscape connectivity alongside reforestation, including protection of existing forest patches and spatially coordinated restoration where appropriate. Planning strategies should also account for the socioeconomic drivers of land-use change and climate-related pressures that may influence the persistence and ecological quality of recovered forests. Future research should combine landscape metrics with species-specific movement data, field-based ecological assessments, and higher-resolution remote sensing to evaluate functional connectivity and the long-term biodiversity outcomes of restoration. The integrated analytical framework applied in this study provides spatial information that may support future conservation and urban environmental planning in Islamabad and comparable rapidly urbanizing landscapes.

Supplementary Materials: The following supporting information can be downloaded at: https://www.mdpi.com/article/10.3390/land15091641/s1, Table S1: Formula and significance of Class and Landscape-level metrics; Table S2: Transition area matrix (TAM) (%) of LULC between 1991–2001, 2001–2011, 2011–2021, and 1991–2021; Table S3: Class-Level Landscape Metrics (1991–2021); Table S4: Transition Dynamics of Forest Fragmentation Classes from 1991 to 2021; Table S5: Sensitivity of 2021 forest-fragmentation classification to different edge thresholds (50 m, 100 m, and 150 m); Figure S1: The square window moves from left to right; Figure S2: Forest and non-forest areas mainly cover the Margalla Hills National Park.

Author Contributions: Conceptualization, M.T.B., H.U.K., M.S., S.R., K.H., F.A., I.D.l.T.D., M.S.G.d.M. and E.S.A.; Methodology, H.U.K., M.S. and K.H.; Software, M.S. and S.R.; Validation, M.T.B.; Formal analysis, M.T.B. and H.U.K.; Investigation, M.T.B., H.U.K., M.S., S.R., K.H., F.A., I.D.l.T.D., M.S.G.d.M. and E.S.A.; Resources, M.S., S.R. and E.S.A.; Data curation, M.S., S.R., K.H., F.A. and E.S.A.; Writing—original draft, M.T.B., H.U.K., S.R., F.A., I.D.l.T.D. and M.S.G.d.M.; Writing—review & editing, M.T.B., H.U.K., S.R., K.H., F.A., M.S.G.d.M. and E.S.A.; Visualization, M.T.B., H.U.K., M.S., S.R., K.H., I.D.l.T.D., M.S.G.d.M. and E.S.A.; Supervision, H.U.K., K.H., F.A. and I.D.l.T.D.; Project administration, M.S.G.d.M. and E.S.A. All authors have read and agreed to the published version of the manuscript.

Funding: This research was funded by Fundación Universidad Europea del Atlántico.

Data Availability Statement: The original contributions presented in the study are included in the article/Supplementary Material, and further inquiries can be directed to the corresponding author.

Acknowledgments: During the preparation of this manuscript, the author used Grammarly and ChatGPT 5.6 for the purposes of language refinement. The authors have reviewed and edited the output and take full responsibility for the content of this publication.

Conflicts of Interest: The authors declare no conflicts of interest.

References

1. Han, L.; Zhou, Z. Identifying the Changes in Ecosystem Services and Human Wellbeing under Agricultural Transformation Contexts in Peri-Urban Areas: A Case Study of the Xi'an Metropolitan Zone, China. *Land* **2024**, *13*, 193. [CrossRef]
2. Yaghoobi, M.; Vafaeenejad, A.; Moradi, H.; Hashemi, H. Analysis of Landscape Composition and Configuration Based on LULC Change Modeling. *Sustainability* **2022**, *14*, 13070. [CrossRef]
3. Choudhury, K.; Jansen, J.M. *Terminology for Intergrated Resources Planning and Management*; FAO: Rome, Italy, 1998.
4. Hendry, A.P.; Gotanda, K.M.; Svensson, E.I. Human influences on evolution, and the ecological and societal consequences. *Philos. Trans. R. Soc. B Biol. Sci.* **2017**, *372*, 20160028. [CrossRef]
5. Li, C.; Qiao, W.; Gao, B.; Chen, Y. Unveiling spatial heterogeneity of ecosystem services and their drivers in varied landform types: Insights from the Sichuan-Yunnan ecological barrier area. *J. Clean. Prod.* **2024**, *442*, 141158. [CrossRef]
6. Liu, J.; Pei, X.; Zhu, W.; Jiao, J. Assessing the influence of simulated environmental gradients on the spatial heterogeneity of landscape patterns in the Tibetan Plateau. *J. Environ. Manag.* **2024**, *359*, 120957. [CrossRef]
7. Duarte, G.T.; Santos, P.M.; Cornelissen, T.G.; Ribeiro, M.C.; Paglia, A.P. The effects of landscape patterns on ecosystem services: Meta-analyses of landscape services. *Landsc. Ecol.* **2018**, *33*, 1247–1257. [CrossRef]
8. Mulatu, K.; Hundera, K.; Senbeta, F. Analysis of land use/land cover changes and landscape fragmentation in the Baro-Akobo Basin, Southwestern Ethiopia. *Heliyon* **2024**, *10*, e28378. [CrossRef]
9. He, Y.; Liu, X.; Wu, D.; Li, S.; Zhou, P. Ecological Risks and Patterns Associated with Land Use/Cover Changes Along the Belt and Road Initiative Routes. *Land Degrad. Dev.* **2025**, *36*, 2075–2094. [CrossRef]
10. Mostafazadeh, R.; Talebi Khiavi, H. Landscape change assessment and its prediction in a mountainous gradient with diverse land-uses: Mostafazadeh and Khiavi. *Environ. Dev. Sustain.* **2024**, *26*, 3911–3941. [CrossRef]
11. Ning, C.; Subedi, R.; Hao, L. Land Use/Cover Change, Fragmentation, and Driving Factors in Nepal in the Last 25 Years. *Sustainability* **2023**, *15*, 6957. [CrossRef]
12. Abuhay, A.; Kassaw, E.; Masresha, G.; Asefa, M. Small forest patches in Ethiopian highlands uniquely support high plant biodiversity. *Biodivers. Conserv.* **2024**, *33*, 1711–1727. [CrossRef]
13. Mengist, W.; Soromessa, T.; Feyisa, G.L. Landscape change effects on habitat quality in a forest biosphere reserve: Implications for the conservation of native habitats. *J. Clean. Prod.* **2021**, *329*, 129778. [CrossRef]
14. Al Mamun, M.M.; Nijhuis, S.; Newton, C. Sustainable Urban Planning Challenges in the Peri-Urban Landscape: Evaluating LULC Dynamics and the Policy Effectiveness of the Chattogram Metropolitan Region, Bangladesh. *Land* **2024**, *13*, 1157. [CrossRef]
15. Pooja Singh, R.; Chauhan, V.; Singh, A.K. Forest Degradation and Deforestation: Drivers and Solution. In *Forestry for a Carbon-Neutral and Sustainable Future: A Scientific Perspective*; Springer Nature: Cham, Switzerland, 2026; pp. 345–369.
16. Koutsias, N.; Panourgia, K.; Nakas, G.; Petanidou, T. The importance of landscape and fire-history as factors explaining post-fire vegetation recovery in a Mediterranean island using Sentinel-2 satellite data. *Sci. Total Environ.* **2024**, *957*, 177443. [CrossRef]
17. Mandal, A.; Mondal, N.S. Cap and Trade System in Agroforestry: A Way to Help Farmers to Mitigate Climate Change Risk. In *Agroforestry for Monetising Carbon Credits*; Springer Nature: Cham, Switzerland, 2025; pp. 575–589. [CrossRef]
18. Adhikari, S.; Bhandari, B.; Sharma, B.P. Evaluating the Impact of Deforestation on Climate Change: A Comparative Analysis of the Amazon and Congo Basins. *Int. Rev. Appl. Res. Technol. Soc. Innov.* **2025**, *15*.

19. Shah, A.; Ali, K.; Nizami, S.M. Four decadal urban land degradation in Pakistan a case study of capital city islamabad during 1979–2019. *Environ. Sustain. Indic.* **2021**, *10*, 100108. [CrossRef]
20. Aziz, A.; Anwar, M.M. Assessing the impacts of urban expansion on sustainability; empirical evidence from Islamabad, Pakistan. *GeoJournal* **2024**, *89*, 82. [CrossRef]
21. Gilani, H.; Ahmad, S.; Qazi, W.A.; Abubakar, S.M.; Khalid, M. Monitoring of urban landscape ecology dynamics of Islamabad capital territory (ICT), Pakistan, over four decades (1976–2016). *Land* **2020**, *9*, 123. [CrossRef]
22. Haq, F.; Mark, B.G.; Shum, C.K.; Zeballos-Castellon, G.; Rahman, G. Effectiveness of billion trees Tsunami afforestation projects in restoration of forests in Pakistan. *Environ. Dev. Sustain.* **2024**, *27*, 25087–25102. [CrossRef]
23. Gu, C. Urbanization: Processes and driving forces. *Sci. China Earth Sci.* **2019**, *62*, 1351–1360. [CrossRef]
24. Pili, S.; Serra, P.; Salvati, L. Landscape and the city: Agro-forest systems, land fragmentation and the ecological network in Rome, Italy. *Urban. For. Urban. Green.* **2019**, *41*, 230–237. [CrossRef]
25. Zhen, S.; Zhao, Q.; Liu, S.; Wu, Z.; Lin, S.; Li, J.; Hu, X. Detecting spatiotemporal dynamics and driving patterns in forest fragmentation with a forest fragmentation comprehensive index (FFCI): Taking an area with active forest cover change as a case study. *Forests* **2023**, *14*, 1135. [CrossRef]
26. Faiytole, A.A.; Adewumi, V.A. Urban expansion and transportation interaction: Evidence from Akure, southwestern Nigeria. *Environ. Plan. B Urban. Anal. City Sci.* **2024**, *51*, 57–74. [CrossRef]
27. Wang, L.; Saiz, A.; Li, W. Natural fragmentation increases urban density but impedes transportation and city growth worldwide. *Nat. Cities* **2024**, *1*, 642–653. [CrossRef]
28. Müller, N.; Ignatieva, M.; Nilon, C.H.; Werner, P.; Zipperer, W.C. Patterns and trends in urban biodiversity and landscape design. In *Urbanization, Biodiversity and Ecosystem Services: Challenges and Opportunities: A Global Assessment*; Springer: Berlin/Heidelberg, Germany, 2013. [CrossRef]
29. Das, M.; Das, A. Assessing the Impact of Master Plan on the Dynamicity and Resilience of Forest Cover Change: A Study on Adina Deer Park (Forest), West Bengal, India. *GeoJournal* **2021**, *86*, 2587–2606. [CrossRef]
30. Saha, A.; Saha, S.; Das, A.; Mandal, S.; Sarkar, R.; Das, M. Unveiling the Landscape Fragmentation and Its Impact on Land Surface Temperature Using Machine Learning Approach in Kolkata Metropolitan Area (India). *Theor. Appl. Climatol.* **2025**, *156*, 384. [CrossRef]
31. Ahmed, N.; Padda, I.U.H.; Khan, A.; Otil, M.D.; Cismas, L.M.; Miculescu, A.; Rehman, A. Climate change adaption strategies in urban communities: New evidence from Islamabad, Pakistan. *Environ. Sci. Pollut. Res.* **2023**, *30*, 42108–42121. [CrossRef]
32. Khurram, A. Problem Identification: Examining the Factors that Resulted in Islamabad's Unsustainable Development. Master's Thesis, Middle East Technical University, Ankara, Turkey, 2022.
33. Pakistan Bureau of Statistics. *Population and Housing Census 2023: District Census Report—Islamabad*; Pakistan Bureau of Statistics: Islamabad, Pakistan. Available online: www.pbs.gov.pk (accessed on 21 August 2026).
34. Khan, D.; Khan, N.; Choudhury, U.; Singh, S.K.; Kanga, S.; Kumar, P.; Meraj, G. Urban expansion and spatial growth patterns in Lucknow: Implications for sustainable development (1991–2021). *Sustainability* **2024**, *17*, 227. [CrossRef]
35. Kamran Khan, J.A.; Khayyam, U.; Waheed, A.; Khokhar, M.F. Exploring the nexus between land use land cover (LULC) changes and population growth in a planned city of islamabad and unplanned city of Rawalpindi, Pakistan. *Heliyon* **2023**, *9*, e13297. [CrossRef]
36. Gkyer, E. Understanding Landscape Structure Using Landscape Metrics. In *Advances in Landscape Architecture*; InTech: London, UK, 2013. [CrossRef]
37. Badshah, M.T.; Hussain, K.; Rehman, A.U.; Mehmood, K.; Muhammad, B.; Wiarta, R.; Silamon, R.F.; Khan, M.A.; Meng, J. The role of random forest and Markov chain models in understanding metropolitan urban growth trajectory. *Front. For. Glob. Change* **2024**, *7*, 1345047. [CrossRef]
38. Fan, Z.; Li, S.; Fang, H. Explicitly identifying the desertification change in CMREC area based on multisource remote data. *Remote Sens.* **2020**, *12*, 3170. [CrossRef]
39. Huang, H.; Chen, W.; Zhang, Y.; Qiao, L.; Du, Y. Analysis of ecological quality in Lhasa Metropolitan Area during 1990–2017 based on remote sensing and Google Earth Engine platform. *J. Geogr. Sci.* **2021**, *31*, 265–280. [CrossRef]
40. Banerjee, A.; Kang, S.; Meadows, M.E.; Xia, Z.; Sengupta, D.; Kumar, V. Quantifying climate variability and regional anthropogenic influence on vegetation dynamics in northwest India. *Environ. Res.* **2023**, *234*, 116541. [CrossRef]
41. Abdi, A.M. Land cover and land use classification performance of machine learning algorithms in a boreal landscape using Sentinel-2 data. *GIScience Remote Sens.* **2020**, *57*, 1–20. [CrossRef]
42. Jin, Y.; Liu, X.; Chen, Y.; Liang, X. Land-cover mapping using Random Forest classification and incorporating NDVI time-series and texture: A case study of central Shandong. *Int. J. Remote Sens.* **2018**, *39*, 8703–8723. [CrossRef]
43. Li, X.; Chen, W.; Cheng, X.; Wang, L. A comparison of machine learning algorithms for mapping of complex surface-mined and agricultural landscapes using ZiYuan-3 stereo satellite imagery. *Remote Sens.* **2016**, *8*, 514. [CrossRef]

44. Shi, Y.; Qi, Z.; Liu, X.; Niu, N.; Zhang, H. Urban land use and land cover classification using multisource remote sensing images and social media data. *Remote Sens.* **2019**, *11*, 2719. [CrossRef]
45. Zhang, F.; Yang, X. Improving land cover classification in an urbanized coastal area by random forests: The role of variable selection. *Remote Sens. Environ.* **2020**, *251*, 112105. [CrossRef]
46. Abdel-Rahman, E.M.; Mutanga, O.; Adam, E.; Ismail, R. Detecting Sirex noctilio grey-attacked and lightning-struck pine trees using airborne hyperspectral data, random forest, and support vector machines classifiers. *ISPRS J. Photogramm. Remote Sens.* **2014**, *88*, 48–59. [CrossRef]
47. Rodriguez-Galiano, V.F.; Chica-Rivas, M. Evaluation of different machine learning methods for land cover mapping of a Mediterranean area using multi-seasonal Landsat images and Digital Terrain Models. *Int. J. Digit. Earth* **2014**, *7*, 492–509. [CrossRef]
48. Brieuc, M.S.O.; Waters, C.D.; Drinan, D.P.; Naish, K.A. A practical introduction to Random Forest for genetic association studies in ecology and evolution. *Mol. Ecol. Resour.* **2018**, *18*, 755–766. [CrossRef]
49. He, Y.; Oh, J.; Lee, E.; Kim, Y. Land Cover and Land Use Mapping of the East Asian Summer Monsoon Region from 1982 to 2015. *Land* **2022**, *11*, 391. [CrossRef]
50. Mishra, V.N.; Rai, P.K. A remote sensing aided multi-layer perceptron-Markov chain analysis for land use and land cover change prediction in Patna district (Bihar), India. *Arab. J. Geosci.* **2016**, *9*, 249. [CrossRef]
51. de Souza, J.M.; Morgado, P.; da Costa, E.M.; de Novaes Vianna, L.F. Modeling of Land Use and Land Cover (LULC) Change Based on Artificial Neural Networks for the Chapecó River Ecological Corridor, Santa Catarina/Brazil. *Sustainability* **2022**, *14*, 4038. [CrossRef]
52. Xue, S.; Ma, B.; Wang, C.; Li, Z. Identifying key landscape pattern indices influencing the NPP: A case study of the upper and middle reaches of the Yellow River. *Ecol. Modell.* **2023**, *484*, 110457. [CrossRef]
53. Masoudi, M.; Richards, D.R.; Tan, P.Y. Assessment of the Influence of Spatial Scale and Type of Land Cover on Urban Landscape Pattern Analysis Using Landscape Metrics. *J. Geovisualization Spat. Anal.* **2024**, *8*, 8. [CrossRef]
54. Yang, X.; Fu, B.; Chen, L. Remote sensing and geospatial analysis for landscape pattern characterization. In *Landscape Ecology for Sustainable Environment and Culture*; Springer: Berlin/Heidelberg, Germany, 2013. [CrossRef]
55. Zhao, Y.; Kasimu, A.; Gao, P.; Liang, H. Spatiotemporal Changes in The Urban Landscape Pattern and Driving Forces of LUCC Characteristics in The Urban Agglomeration on The Northern Slope of The Tianshan Mountains from 1995 to 2018. *Land* **2022**, *11*, 1745. [CrossRef]
56. McGarigal, K. *FRAGSTATS HELP v4: Spatial Pattern Analysis Program for Categorical and Continuous Maps. Computer software programs produced by the authors at the University of Massachusetts, Amherst*; LandEco Consulting: Warriewood, NSW, Australia, 2015. Available online: https://www.fragstats.org/index.php/background/what-is-a-landscape (accessed on 21 August 2026).
57. Bosch, M.; Jaligot, R.; Chenal, J. Spatiotemporal patterns of urbanization in three Swiss urban agglomerations: Insights from landscape metrics, growth modes and fractal analysis. *Landsc. Ecol.* **2020**, *35*, 879–891. [CrossRef]
58. Lam, N.S.N.; Cheng, W.; Zou, L.; Cai, H. Effects of landscape fragmentation on land loss. *Remote Sens. Environ.* **2018**, *209*, 253–262. [CrossRef]
59. Hagen-Zanker, A. A computational framework for generalized moving windows and its application to landscape pattern analysis. *Int. J. Appl. Earth Obs. Geoinf.* **2016**, *44*, 205–216. [CrossRef]
60. Carneiro, L.d.S.; de Aguiar, W.M.; Priante, C.d.F.; Ribeiro, M.C.; Frantine-Silva, W.; Gaglianone, M.C. The Interplay Between Thematic Resolution, Forest Cover, and Heterogeneity for Explaining Euglossini Bees Community in an Agricultural Landscape. *Front. Ecol. Evol.* **2021**, *9*, 628319. [CrossRef]
61. Mengist, W.; Soromessa, T.; Feyisa, G.L. Forest fragmentation in a forest Biosphere Reserve: Implications for the sustainability of natural habitats and forest management policy in Ethiopia. *Resour. Environ. Sustain.* **2022**, *8*, 100058. [CrossRef]
62. Zheng, L.; Wang, Y.; Li, J. Quantifying the spatial impact of landscape fragmentation on habitat quality: A multi-temporal dimensional comparison between the Yangtze River Economic Belt and Yellow River Basin of China. *Land Use Policy* **2023**, *125*, 106463. [CrossRef]
63. Huang, Y.; Zheng, M.; Li, T.; Xiao, F.; Zheng, X. An Integrated Framework for Landscape Indices' Calculation with Raster–Vector Integration Its Application Based on Q.G.I.S. *ISPRS Int. J. Geoinf.* **2024**, *13*, 242. [CrossRef]
64. Jung, M. LecoS—A python plugin for automated landscape ecology analysis. *Ecol. Inform.* **2016**, *31*, 18–21. [CrossRef]
65. Zhang, Y.; Shen, W.; Li, M.; Lv, Y. Assessing spatio-temporal changes in forest cover and fragmentation under urban expansion in Nanjing, eastern China, from long-term Landsat observations (1987–2017). *Appl. Geogr.* **2020**, *117*, 102190. [CrossRef]
66. Rempel, R.S.; Kaukinen, D.; Carr, A.P. *Patch Analyst and Patch Grid. Ontario Ministry of Natural Resources*; Centre for Northern Forest Ecosystem Research: Thunder Bay, ON, Canada, 2012.
67. Center for Land Use Education and Research (CLEAR). Landscape Fragmentation Tools (LFT) v2.0. University of Connecticut. Available online: https://clear.uconn.edu (accessed on 21 August 2026).

68. Rahman, M.; Jashimuddin, M.; Kamrul, I.; Kumar Nath, T. Land Use Change and Forest Fragmentation Analysis: A Geoinformatics Approach on Chunati Wildlife Sanctuary, Bangladesh. *J. Civil. Eng. Environ. Sci.* **2016**, *2*, 20–29. [CrossRef]
69. Shimrah, T.; Lungleng, P.; Devi, A.R.; Sarma, K.; Varah, F.; Khuman, Y.S. Spatio-temporal assessment of land use and land cover (LULC) and forest fragmentation in the shifting agroecosystem landscape in the Ukhrul district of Manipur, Northeast India. *Environ. Monit. Assess.* **2022**, *194*, 14. [CrossRef]
70. Randhawa, K.; Bhattacharya, P.; Shimrah, T. Spatio-temporal analysis of urban forest fragmentation in Delhi, India, using Landscape Fragmentation Tool v2. 0. *Environ. Monit. Assess.* **2024**, *196*, 1273. [CrossRef]
71. Abbas, Z.; Zhu, Z.; Zhao, Y. Spatiotemporal analysis of landscape pattern and structure in the Greater Bay Area, China. *Earth Sci. Inform.* **2022**, *15*, 1977–1992. [CrossRef]
72. Arshad, S.; Ahmad, S.R.; Abbas, S.; Asharf, A.; Siddiqui, N.A.; Islam, Z.U. Quantifying the contribution of diminishing green spaces and urban sprawl to urban heat island effect in a rapidly urbanizing metropolitan city of Pakistan. *Land Use Policy* **2022**, *113*, 105874. [CrossRef]
73. Sabir, M.; Ali, Y.; Khan, I.; Salman, A. Plants Species Selection for Afforestation: A Case Study of the Billion Tree Tsunami Project of Pakistan. *J. Sustain. For.* **2022**, *41*, 105874. [CrossRef]
74. Hussain, K.; Badshah, T.; Mehmood, K.; Rahman, A.U.; Shahzad, F.; Anees, S.A.; Khan, W.R.; Yujun, S. Comparative analysis of sensors and classification algorithms for land cover classification in Islamabad, Pakistan. *Earth Sci. Inform.* **2025**, *18*, 212. [CrossRef]
75. Sarkar, S.; Mallick, S.K.; Manna, H.; Roy, S.K. Urbanization-Induced land use dynamics and its impacts on present and future urban ecosystem services in the industrial cities of India. *Earth Syst. Environ.* **2024**, *8*, 869–893. [CrossRef]
76. Rahman, F.; Rahman, M.T.U. Use of cellular automata-based artificial neural networks for detection and prediction of land use changes in North-Western Dhaka City. *Environ. Sci. Pollut. Res.* **2023**, *30*, 1428–1450. [CrossRef]
77. Andrieu, J.; Anupama, K.; Bautes, N.; Benabou, S.; Crook, O.J.; Gunasekera, V.; Jayasingam, T.; Jayathilaka, C.; Kodikara, K.A.S.; Lombard, F.; et al. Multiscale analysis of land use and land cover changes in Sri Lanka by remote sensing: The impacts of post-war infrastructure development in the last 20 Years (2002–2022). *J. Natl. Sci. Found.* **2023**, *51*, 675–688. [CrossRef]
78. Shiraishi, K.; Terada, T. Tokyo's urban tree challenge: Decline in tree canopy cover in Tokyo from 2013 to 2022. *Urban Urban Green* **2024**, *97*, 128331. [CrossRef]
79. Yang, H.; Zhong, X.; Deng, S.; Nie, S. Impact of LUCC on landscape pattern in the Yangtze River Basin during 2001–2019. *Ecol. Inform.* **2022**, *69*, 101631. [CrossRef]
80. Hussain, M.F.; Meng, X.; Shah, S.F.; Hussain, M.A. Integrating Spatiotemporal Analysis of Land Transformation and Urban Growth in Peshawar Valley and Its Implications on Temperature in Response to Climate Change. *ISPRS Int. J. Geoinf.* **2024**, *13*, 239. [CrossRef]
81. Sarwar, S.; Khan, H.U.A.; Wu, F.; Hasan, S.; Zohaib, M.; Abbasi, M.; Hu, T. Forecasting Urban Sprawl Dynamics in Islamabad: A Neural Network Approach. *Remote Sens.* **2025**, *17*, 492. [CrossRef]
82. Yuan, Z.; Zhou, L.; Sun, D.; Hu, F. Impacts of Urban Expansion on the Loss and Fragmentation of Cropland in the Major Grain Production Areas of China. *Land* **2022**, *11*, 130. [CrossRef]
83. Ding, Z.D.; Sun, Z.; Xie, Y.H.; Qiao, J.J.; Liang, R.T.; Chen, X.; Hussain, K.; Sun, Y.J. Optimizing crown density and volume estimation across two coniferous forest types in southern China via Boruta and Cubist methods. *J. Plant Ecol.* **2024**, *17*, rtae039. [CrossRef]
84. Imbrenda, V.; Quaranta, G.; Salvia, R.; Egidi, G.; Salvati, L.; Prokopovà, M.; Coluzzi, R.; Lanfredi, M. Land degradation and metropolitan expansion in a peri-urban environment. *Geomat. Nat. Hazards Risk* **2021**, *12*, 1797–1818. [CrossRef]
85. Jiayu, C.; Jiefu, X.; Kang, G.; Yiwu, W. Balancing urban expansion with ecological integrity: An ESP framework for rapidly urbanizing small and medium-sized cities, with insights from Suizhou, China. *Ecol. Inform.* **2024**, *80*, 102508. [CrossRef]
86. Soh, M.C.K.; Mitchell, N.J.; Ridley, A.R.; Butler, C.W.; Puan, C.L.; Peh, K.S.H. Impacts of Habitat Degradation on Tropical Montane Biodiversity and Ecosystem Services: A Systematic Map for Identifying Future Research Priorities. *Front. For. Glob. Change* **2019**, *2*, 83. [CrossRef]

Disclaimer/Publisher's Note: The statements, opinions and data contained in all publications are solely those of the individual author(s) and contributor(s) and not of MDPI and/or the editor(s). MDPI and/or the editor(s) disclaim responsibility for any injury to people or property resulting from any ideas, methods, instructions or products referred to in the content.